



Published in final edited form as:

Cell Death Differ. 2009 October ; 16(10): 1385–1394. doi:10.1038/cdd.2009.88.

***C. elegans* caspase homolog CSP-2 inhibits CED-3 autoactivation and apoptosis in germ cells**

X Geng^{1,4}, QH Zhou^{1,4}, E Kage-Nakadai², Y Shi³, N Yan³, S Mitani², and D Xue^{1,*}

¹ Department of Molecular, Cellular, and Developmental Biology, Campus Box 347, University of Colorado, Boulder, CO 80309, USA

² Department of Physiology, Tokyo Women's Medical University, School of Medicine, and CREST, JST, 8-1, Kawada-cho, Shinjuku-ku, Tokyo, 162-8666, Japan

³ Center for Structural Biology, Institute of Biomedicine, Tsinghua University, Beijing, 100084, China

Abstract

In *C. elegans*, apoptosis in germ cells is mediated by the same core apoptotic machinery that controls apoptosis in somatic cells. These include the CED-3 caspase, the CED-3 activator CED-4, and the cell death inhibitor CED-9. However, germline apoptosis also differs from somatic apoptosis in its regulation. We found that CSP-3, a caspase homolog that blocks CED-3 autoactivation and apoptosis in somatic cells, does not affect apoptosis in germ cells. Interestingly, the second *C. elegans* caspase homolog CSP-2 shares sequence similarity to both catalytic subunits of the CED-3 caspase, and surprisingly, contains a stretch of sequence that is almost identical to that of CSP-3. Unlike CSP-3 that acts specifically in somatic cells, loss of CSP-2 causes increased apoptosis only in germ cells, suggesting that CSP-2 is a germ cell specific apoptosis inhibitor. Moreover, like CSP-3, CSP-2 associates with the CED-3 zymogen and inhibits its autoactivation, but does not inhibit CED-4-induced CED-3 activation or the activity of the activated CED-3 protease. Thus, two different *C. elegans* caspase homologs employ the same mechanism to prevent caspase autoactivation and apoptosis in different tissues, suggesting that this could be a generally applicable strategy for regulating caspase activation and apoptosis.

Keywords

germ cell death; *Caenorhabditis elegans*; CED-3; caspase activation; cell death inhibitor

In *Caenorhabditis elegans*, many early developing germ cells undergo apoptosis during normal oogenesis; this process is called germline apoptosis^{1, 2}. Germline apoptosis appears to be an integral component of the oogenesis program and has been suggested to be important for eliminating excess germ cells that acted as nurse cells to provide cytoplasmic

Users may view, print, copy, and download text and data-mine the content in such documents, for the purposes of academic research, subject always to the full Conditions of use:http://www.nature.com/authors/editorial_policies/license.html#terms

*Corresponding author: Dr. D Xue, Department of Molecular, Cellular, and Developmental Biology, Campus Box 347, University of Colorado, Boulder, CO 80309, USA. Tel: 303 492 0271, Fax: 303 492 7744, ding.xue@colorado.edu.

⁴These two authors contributed equally to this work.

components to maturing oocytes^{1–3}. Germline apoptosis is conserved among eukaryotes, from *C. elegans* to humans. Therefore, *C. elegans* provides an excellent model system for studying the regulation of germ cell apoptosis.

The molecular machinery that mediates germline apoptosis has been extensively studied and found to share key components with that of somatic apoptosis. In particular, CED-3, CED-4 and CED-9 are essential for apoptosis in both germ cells and somatic cells^{1, 2}. However, regulation of apoptosis in germ cells and in somatic cells appears to differ significantly. For example, the pro-apoptotic BH3 only protein EGL-1 is crucial for somatic apoptosis but is dispensable for physiological germ cell death¹. Moreover, *C. elegans* somatic cells are resistant to genotoxic insults, whereas germ cells readily respond to genotoxic stresses to undergo apoptosis⁴, suggesting that the regulation of germ cell death could be fundamentally different from that of somatic cell death.

One crucial aspect of apoptosis regulation is the regulation of caspases, the aspartate-specific cysteine proteases that execute the cell killing process^{5, 6}. Numerous caspase inhibitors have been identified and shown to inhibit the activation or the activities of caspases. In particular, the inhibitor of apoptosis proteins (IAPs), characterized by at least one baculoviral IAP repeat (BIR) and a RING finger motif⁷, are conserved caspase inhibitors in *Drosophila* and higher organisms^{8–12}. However, no IAP homolog has been identified in *C. elegans*. Instead, a partial caspase homolog CSP-3 was found to protect *C. elegans* somatic cells from apoptosis by associating with the CED-3 zymogen and inhibiting CED-3 autoactivation¹³. It is unclear whether CSP-3 also inhibits CED-3 autoactivation in *C. elegans* germ cells and how the activity of CED-3 is negatively regulated in the germline.

In this study, we found that a second *C. elegans* caspase homolog CSP-2, which shares sequence similarity to both catalytic subunits of CED-3 (Figure 1a), is expressed specifically in the *C. elegans* germline and acts as a germ-cell-specific cell death inhibitor. Moreover, CSP-2 associates with the CED-3 zymogen and specifically inhibits CED-3 autoactivation, but not CED-3 activation mediated by CED-4 or CED-3's catalytic activity. Our findings suggest that caspase homologs lacking protease activities serve as dedicated caspase inhibitors in *C. elegans* to prevent CED-3 from inadvertent autoactivation and cells from apoptosis.

Results

Loss of *csp-2* causes increased germ cell death but does not affect somatic cell death

CSP-2 was first identified as a caspase homolog that shares sequence similarity to both catalytic subunits of CED-3 (Figure 1a). However, CSP-2 does not appear to contain a caspase activity *in vitro*¹⁴, probably because it lacks the invariant active-site pentapeptide QACXG (X could be R, Q, or G) found in all active caspases (VCCRG in CSP-2)¹⁵. Interestingly, the carboxyl terminal region of CSP-2 is homologous to the small subunit of CED-3 and shares 92% identity to CSP-3 (Figure 1a), raising an intriguing possibility that CSP-2 may act as a caspase inhibitor like CSP-3. To examine the function of *csp-2* in *C. elegans*, we obtained three different *csp-2* deletion alleles (Figure 1b). Two deletions, *tm2858* and *tm3077*, remove parts of the carboxyl terminal region of CSP-2, which is

present in both *csp-2* transcripts identified previously (Figure 1b)¹⁴. These two *csp-2* transcripts conceptually encode two proteins, CSP-2A and CSP-2B, respectively. CSP-2B is identical to the carboxyl terminus of CSP-2A, which has an extra 563 amino acid at the amino terminus. Since CSP-2B transcript is trans-spliced to the SL1 spliced leader, it is an independent, complete transcript^{14, 16}. Indeed, RT-PCR analysis of mixed stage wild-type animals reveals that CSP-2B is the dominant *csp-2* message and we barely detected any CSP-2A transcript (Figure 1c). Moreover, in western blot analysis, we only detected a protein of approximately 33 kDa, the size of CSP-2B, in worm lysate derived from animals carrying a complex transgene array expressing CSP-2::3xFlag under the control of its own promoter ($P_{csp-2}csp-2::3xFlag$; Figure 1b and 1d). These results indicate that CSP-2B is the major CSP-2 protein expressed in *C. elegans*, although very low-level expression of CSP-2A cannot be ruled out. The third deletion, *ok1742*, specifically removes a region in CSP-2A but does not affect the CSP-2B coding region.

To investigate whether *csp-2* affects apoptosis, we counted the number of apoptotic cells in the germline and embryos of *csp-2* deletion mutants, two developmental stages with active apoptosis events. Since apoptotic cells are swiftly engulfed in *C. elegans*, we sensitized these cell corpse assays by counting *ced-6(n2095)*; *csp-2* and *ced-2(n1994)* *csp-2* double mutants, in which cell corpse engulfment is disabled due to the inactivation of the *ced-2* or the *ced-6* gene and a small increase in cell death will result in a greater increase in the number of persistent cell corpses^{13, 17}. Unlike the *csp-3(tm2260)* mutation that causes increased cell deaths in *C. elegans* embryos and ectopic deaths of neurons that normally live¹³, *csp-2(tm2858)* and *csp-2(tm3077)* do not seem to affect embryonic cell deaths (Figure 2a and b) or result in missing touch cells in larvae (Figure 2c; data not shown), suggesting that *csp-2* does not affect apoptosis in somatic tissues. However, we did observe a slight increase in germ cell deaths in *csp-2(tm2858)* and *csp-2(tm3077)* animals compared with wild-type animals (Figure 3a; data not shown) and the increase in germ cell corpses is easily detected in the *ced-6(n2095)* and *ced-2(n1994)* mutant backgrounds (Figure 3b to 3e), suggesting that loss of *csp-2* causes increased germ cell deaths and that CSP-2 inhibits apoptosis in germ cells. By contrast, we did not observe increased germ cell corpses in *csp-3(tm2260)*, *csp-3(tm2260)*; *ced-6(n2095)*, or *csp-3(tm2260)*; *ced-2(n1994)* animals, compared with wild-type, *ced-6(n2095)*, and *ced-2(n1994)* animals, respectively (Figure 3a, c and e). Nor did we observe further increase in germ cell deaths in the *csp-3(tm2260)*; *csp-2(tm3077)* double mutant or in the *csp-3(tm2260)*; *ced-6(n2095)*; *csp-2(tm3077)* and *csp-3(tm2260)*; *ced-2(n1994)* *csp-2(tm3077)* triple mutants (Figure 3a, c, and e), indicating that *csp-3* does not contribute to the inhibition of germ cell death. Interestingly, unlike *csp-2(tm2858)* and *csp-2(tm3077)* deletion mutations, *csp-2(ok1742)*, which removes only the CSP-2A coding region, did not seem to affect germ cell death (Figure 3c). This result is consistent with our observations that the CSP-2B transcript is the dominant *csp-2* transcript in *C. elegans* and suggests that CSP-2B is mainly responsible for inhibiting germ cell death in the *csp-2* locus and that CSP-2A is not critical for this inhibitory function. We thus only analyzed the activity of CSP-2B hereafter.

Loss of *csp-2* reduces animal brood size

We also examined whether ectopic deaths of germ cells in *csp-2(lf)* mutants affect the brood size of the animals, as what has been observed in animals deficient in *ced-9*, another anti-apoptosis gene¹⁸. Both *csp-2* mutants (*tm3077* and *tm2858*) had significantly reduced brood sizes, approximately 60% of that observed in wild-type animals (Table 1). On the other hand, the *csp-2(ok1742)* mutant, which did not display ectopic germ cell deaths, had a normal brood size (Figure 3c). Moreover, *csp-2(tm3077)* exacerbated the sterility defect caused by a weak loss-of-function mutation in *ced-9 (n1653ts)*¹⁸, resulting in complete sterility of the *ced-9(n1653ts); csp-2(tm3077)* double mutant (Table 1). These results suggest that *csp-2* is important for normal germline development in *C. elegans*.

CSP-2B is specifically expressed in *C. elegans* germline

We next examined the expression patterns of *csp-2* by constructing a CSP-2 translational GFP fusion under the control of its own promoter ($P_{csp-2csp-2::gfp}$) and generating a low-copy integrated transgene (*smIs372*) carrying $P_{csp-2csp-2::gfp}$ through biolistic bombardment (Figure 1b)¹⁹. *smIs372* fully rescued the increased germ cell corpse phenotype of the *ced-2(n1994) csp-2(tm3077)* mutant (Figure 3g), suggesting that the fusion protein is expressed in the right cells and targeted to the appropriate cellular locations. Using an antibody to GFP, we detected CSP-2::GFP in the cytoplasm of all germ cells of *smIs372* hermaphrodite animals but failed to see any GFP staining in somatic cells (Figure 1e and data not shown). This cytoplasmic staining pattern of CSP-2::GFP is similar to that of CSP-3::GFP¹³, suggesting that both proteins act in cytoplasm to inhibit apoptosis. Interestingly, in immunoblotting analysis of worm lysate from male or hermaphrodite animals carrying the $P_{csp-2csp-2::3xFlag}$ complex array, we detected expression of CSP-2B only in hermaphrodites but not in males (Figure. 1d). Since no cell death occurs in male germline^{1, 2}, expression of CSP-2 may be dispensable in males.

To verify that germline expression of CSP-2B is sufficient to mediate the *csp-2* function, we expressed a GFP::CSP-2B fusion under the control of the *pie-1* promoter ($P_{pie-1}GFP::CSP-2B$) in complex transgene arrays that allow expression of transgenes in the germline²⁰. $P_{pie-1}GFP::CSP-2B$ fully rescued the increased germ cell corpse phenotype of the *ced-6(n2095); csp-2(tm3077)* mutant, whereas a mutant $P_{pie-1}GFP::CSP-2B(W131E, L132R, F186D)$ construct failed to do so (Figure 3f; see below), confirming that CSP-2B is responsible for the *csp-2* activity in inhibiting germ cell deaths. We could also rescue the *csp-2(lf)* defect or even cause mild suppression of germ cell deaths by ubiquitously overexpressing CSP-2B under the control of the heat-inducible promoter ($P_{hsp}csp-2B$) from a low-copy transgene (*smIs389*) generated by biolistic bombardment (Figure 3g). Moreover, the $P_{hsp}csp-2B$ transgenes could rescue the missing cell defect of the *csp-3(lf)* mutant in somatic cells (Figure 3h)¹³. However, like CSP-3¹³, overexpression of CSP-2B in soma did not obviously suppress the death of somatic cells that are programmed to die (data not shown). These results indicate that *csp-2* may use a similar mechanism like *csp-3* to prevent cell death.

CSP-2B associates with the CED-3 zymogen

Because CSP-2B shares sequence similarity to both the large and the small subunits of CED-3 that form the active p17/p13 heterodimeric protease complex (Figure 1a)²¹, we tested whether CSP-2B may associate with CED-3 *in vitro* like CSP-313. Using a glutathione S transferase (GST) fusion protein pull-down assay, the CED-3 zymogen tagged with a Flag epitope was pulled down by the GST-CSP-2B fusion, when both were co-expressed in bacteria (Figure 4a). By contrast, the GST control protein failed to do so, suggesting that CSP-2 interacts with the CED-3 zymogen. We then characterized the interaction between CSP-2B and different domains of CED-3 and found that the large subunit (p17) and the small subunit (p13) of CED-3 each could associate with CSP-2B specifically (Figure 4b). Therefore, CSP-2B may interfere with the function of CED-3 by binding to either region of the CED-3 zymogen.

To identify interface residues that are important for CSP-2B binding to CED-3, we constructed a three-dimensional structural model of the CED-3/CSP-2 complex based on the crystal structure of active caspase-3 (Figure 4c)²². We then mutated several potential interface residues and examined whether these mutations interfered with the binding of CSP-2B to CED-3 (data not shown). We found that Trp131 and Leu132, two residues in a CSP-2B region homologous to the large subunit of CED-3, were required for CSP-2B binding to the small subunit of CED-3 (Figure 1a and bottom panel of Figure 4b). On the other hand, Phe186 situated in a CSP-2B region homologous to the small subunit of CED-3 was important for CSP-2B binding to the large subunit of CED-3 *in vitro* (Figure 1a and the upper panel of Figure 4b). Moreover, a CSP-2B mutant carrying these three amino acid substitutions (W131E, L132R, F186D) did not bind CED-3 zymogen (Figure 4a) and failed to rescue the *csp-2(tm3077)* mutant when expressed under the control of the *pie-1* promoter [*P_{pie-1}*GFP::CSP-2B(W131E, L132R, F186D)]; Figure 3f]. These results suggest that association of CSP-2B with CED-3 is important for CSP-2B to protect germ cells from apoptosis.

CSP-2B inhibits specifically autoactivation of the CED-3 zymogen

Since CSP-3 inhibits apoptosis by specifically blocking autoactivation of the CED-3 zymogen, we examined whether CSP-2B has a similar activity using an *in vitro* CED-3 autoactivation assay described previously¹³. As shown in Figure 5a (lanes 1–3), CED-3 zymogen synthesized in rabbit reticulocyte lysate and labeled with ³⁵S-Methionine was slowly auto-processed into active forms. The autoactivation of the CED-3 zymogen was inhibited by the addition of the GST CSP-2B protein (Figure 5a, lanes 4–6) but was not affected by the addition of a similar amount of the GST CSP-2B(W131E, L132R, F186D) protein or the GST protein (Figure 5a, lanes 1–3 and 7–9). Addition of oligomeric CED-4 to the reactions expedited the activation of the CED-3 zymogen (compare lanes 1–5 and lanes 6–10 in Figure 5b). Although GST-CSP-2B completely inhibited CED-3 autoactivation (Figure 5b, lanes 11–15), it delayed but did not block the activation of CED-3 induced by oligomeric CED-4 (Figure 5b, lanes 16–20). GST-CSP-2B also failed to inhibit the catalytic activity of the active CED-3 protease (Figure 5c). Therefore, CSP-2B acts exactly like CSP-3: it complexes with the CED-3 zymogen and inhibits its autoactivation, but is unable to block CED-4-induced CED-3 activation or the activity of active CED-3.

Discussion

Apoptosis is a common feature of metazoan germline development. A wild-type *C. elegans* hermaphrodite has approximately 2000 germ cells generated during its lifetime and more than half of these cells undergo apoptosis in a random fashion¹. By contrast, somatic cell deaths in *C. elegans* occur strictly based on cell lineage information and are invariant from animal to animal²³. As such, these two apoptotic processes likely will be controlled through very different regulatory pathways. Indeed, the cell death initiator EGL-1 that is critical for somatic apoptosis is totally dispensable for physiological germ cell death¹ and it is unclear how germ cell deaths are initiated. Moreover, in this study, we showed that the CED-3 caspase inhibitor CSP-3 does not affect germ cell death (Figure 3c and 3e), providing further evidence that key regulatory components of germ cell death differ from those of somatic cell death to achieve tissue specificity. This finding also suggests that germ cells might possess an alternative CED-3 caspase inhibitor(s) to prevent inappropriate or excessive germ cell deaths.

CSP-2 is the second caspase homolog identified in *C. elegans* and shares sequence similarity to both the large and the small subunits of CED-3¹⁴. However, unlike CSP-1, another worm caspase homolog that possesses a caspase activity¹⁴, CSP-2 does not display any caspase activity *in vitro*, which may result from its lack of the invariant pentapeptide found in active sites of all active caspases¹⁵. Intriguingly, the carboxyl terminus of CSP-2 is 92% identical to CSP-3. Phylogenetic analysis of *C. elegans* CED-3 and CSP proteins suggests that *csp-2* and *csp-3* may have evolved from a common ancestor (Supplementary Figure 1). Therefore, CSP-2 may behave like CSP-3 in binding to CED-3 and inhibiting CED-3 autoactivation¹³. However, inactivation of *csp-2* does not appear to affect somatic cell death, nor does it enhance the *csp-3(lf)* defect in somatic cells (Figure 2), indicating that *csp-2* does not affect apoptosis in somatic cells. On the other hand, inactivation of *csp-2* does increase apoptosis in germ cells (Figure 3), which is not affected by loss of *csp-3*, suggesting that CSP-2, but not CSP-3, acts specifically in germ cells to inhibit apoptosis. Consistent with these findings, CSP-2 is specifically expressed in the *C. elegans* germline. Therefore, CSP-2 and CSP-3, two closely related paralogs, somehow diverge during evolution to act in germ cells and somatic cells, respectively, to inhibit apoptosis, leading to tissue-specific cell death regulation.

Given the unique mode by which CSP-3 regulates CED-3 autoactivation and somatic apoptosis¹³, we tested how CSP-2 inhibits cell death. Our biochemical analysis indicates that CSP-2 directly associates with the CED-3 zymogen through both its small and large subunits (Figure 4a and b). Three amino acid substitutions in CSP-2 (W131E, L132R, F186D) almost completely abolish the binding of CSP-2 to the CED-3 zymogen *in vitro* (Figure 4a) and the apoptosis inhibitory activity of CSP-2 *in vivo* (Figure 3f), suggesting that binding of CSP-2 to CED-3 is critical for its anti-apoptosis function. Moreover, we found that CSP-2 acts exactly like CSP-3 in regulating the activity of CED-3: it associates with the CED-3 zymogen and inhibits its autoactivation, but is unable to block oligomeric CED-4-induced CED-3 activation or inhibit the catalytic activity of activated CED-3 protease (Figure 5a–c). These results establish CSP-2 as the second caspase inhibitor in *C.*

elegans that acts specifically to inhibit autoactivation of CED-3 in germ cells, thereby preventing inappropriate germ cell deaths.

It is interesting that two different caspase homologs employ the same strategy to inhibit CED-3 activation and apoptosis in two different tissues, somatic cells and germ cells (Figure 5d). The repeated use of this unique strategy to negatively regulate CED-3 caspase activation underscores the importance of keeping caspases in check in living cells. In the absence of other obvious caspase inhibitors such as IAPs in *C. elegans*, such caspase-like inhibitors are important players in modulating the level of CED-3 activation and preventing inadvertent CED-3 activation in cells that should live, without interfering with normal cell death induced by CED-4 (Figure 5d), as CSP-2B only delayed but did not block CED-4-induced CED-3 activation (Figure 5b). We propose that similar incomplete or inactive caspase homologs exist in other organisms and could employ the same mechanism to negatively regulate caspase activation and apoptosis.

Materials and Methods

C. elegans strains

We cultured strains of *C. elegans* at 20°C using standard protocols²⁴. The Bristol strain N2 was used as the wild type strain. Most of the alleles including *ced-2(n1994)* and *ced-6(n2095)* used in this study have been described previously²⁵, except *csp-2(tm3077)*, *csp-2(tm2858)*, *csp-2(ok1742)*, and *bzIs8*. The *csp-2(ok1742)* mutant was obtained from *Caenorhabditis* Genetics Center (CGC) and described in Wormbase (<http://www.wormbase.org>). *bzIs8* is an integrated transgene located on LG X and contains a $P_{mec-4}gfp$ construct²⁶, which directs GFP expression in six *C. elegans* touch receptor neurons. All strains were backcrossed with N2 animals 4–10 times prior to analysis.

Quantification of germline apoptosis

We identified and quantified germ cell corpses based on their characteristic morphology when viewed with Nomarski optics as previously described¹. Germline apoptosis was assessed in staged adult animals. At least 15 animals were scored for each time point. Data are reported as mean number of germline cell corpses \pm standard error of the mean (s.e.m).

Isolation of *csp-2(tm3077)* and *csp-2(tm2858)* deletion alleles

We isolated the *csp-2(tm3077)* and *csp-2(tm2858)* deletion alleles from TMP/UV mutagenized worms²⁷. Nested primers used to screen for the *csp-2(tm3077)* and *csp-2(tm2858)* alleles by PCR were 5' GCCGGGCTATCATAATTAAC 3' and 5' ATACTGATCACCGAGGCCAT 3' for the first round amplification and 5' ACGTTTGGGATATCAGTCGA' and 5' CACGTCATTTCTAGACGTCG 3' for the second round amplification. Both mutants were backcrossed with wild-type (N2) animals at least 4 times before they were analyzed further.

RNA isolation and RT-PCR analysis of *csp-2* transcripts

We isolated poly(A)ⁿ mRNA from mix-stage wild-type hermaphrodite animals treated with TRIzol reagent (Invitrogen). First-strand cDNA was reverse-transcribed by using

Superscript III kit (Invitrogen). PCR was performed using specific primers (*csp-2A*, 5' GAGCAGTATAGTGC GTT GAGA-GAG 3' and 5' CTTCTCTCCCTTTCTCTCTGT 3'; *csp-2B*, 5' ACGTTTGGGA-TATCAGTCGA 3' and 5' CTAGACGT CGAAGAATAGTTG 3'), which produce a 706 bp (*csp-2A*) and a 622 bp (*csp-2B*) cDNA fragment, respectively. The PCR products were resolved on a 1.5% agarose gel.

Quantification of somatic apoptotic cell corpses and cells labeled with GFP

We counted cell corpses in animals at various embryonic and larval stages using Nomarski optics as previously described¹³. Also we quantified touch receptor neuron cells in *bzIs8* as previously described¹³.

Plasmids and transgenic strains

We generated the $P_{csp-2csp-2}::gfp$ fusion construct by inserting a *csp-2* genomic fragment containing 4175 bp sequence upstream of the CSP-2A initiation ATG codon and the whole *csp-2* coding region into the pPD95.79 vector. The resulting plasmid was introduced into *ced-1(e1735); unc-119(ed3)* by the microparticle bombardment together with a marker plasmid MM016B that contains the wild-type *unc-119* gene to obtain a low-copy integrated array *smIs37219*. To examine the expression patterns of CSP-2::GFP, anti-GFP immunostaining was carried out on the exposed gonads and embryos of *smIs372* animals²⁸.

We also generated the $P_{pie-1}GFP::CSP-2B$ fusion construct by inserting the full-length *csp-2B* cDNA into pTE5 vector ($P_{pie-1}GFP$) through *SpeI* and *ApaI* site. The $P_{pie-1}GFP::CSP-2B$ fusion construct (wild-type or mutant with W131E, L132R, F186D substitutions) was introduced into the *ced-6(n2095); csp-2(tm3077)* animals through complex DNA arrays as previously described²⁹ and examined for rescue of increased germ cell death phenotype.

Expression and purification of the CSP-2B and CED-3 proteins

We generated all protein expression constructs using the standard PCR-based cloning strategy and verified the clones through sequencing. CSP-2B and CED-3 proteins were expressed either individually or together in *Escherichia coli* strain BL21(DE3) as a N-terminally GST fusion protein and a C-terminally Flag-tagged protein using a pET-41b vector and a pET-3a vector (Novagen), respectively. The soluble fraction of the *E. coli* lysate expressing GST-CSP-2B proteins was purified using a Glutathione Sepharose column and eluted with 10 mM reduced glutathione (Amersham).

GST fusion protein pull-down assays

The GST-CSP-2B fusion protein (wild-type or mutants) or GST was co-expressed with CED-3-Flag, CED-3p13-Flag, or Flag-CED-3p17 in BL21(DE3). Bacteria were lysed by sonication in the lysis buffer [50 mM Tris at pH 8.0, 0.5 mM EDTA, 150mM NaCl, 0.01% (v/v) Triton X-100, and 0.5 mM sucrose] with protease inhibitors and the soluble fraction was incubated with Glutathione Sepharose beads at 4°C for 2 h. The Sepharose beads were then washed five times with the same buffer before the proteins were resolved on a 15%

SDS polyacrylamide gel (SDS-PAGE), transferred to a PVDF membrane, and detected by immunoblotting with an anti-Flag antibody (Sigma).

***In vitro* CED-3 zymogen activation assay**

The CED-3 zymogen was first synthesized and labeled with ³⁵S-Methionine in the TNT Transcription/Translation coupled system (Promega) at 30°C as described previously³⁰, in the presence of equal amount of GST-CSP-2B, GST-CSP-2B(W131E,L132R,F186D), or GST. An aliquot of the reaction was taken out at different time points and mixed with SDS sampling buffer to stop the reaction. For CED-4-mediated CED-3 activation assay, oligomeric CED-4 was added 20 minutes after the initiation of the translation reaction. An aliquot of the reaction was then taken out at different time points and mixed with SDS sampling buffer to stop the reaction. All samples were resolved by 15% SDS PAGE and analyzed by autoradiography.

Statistics

We performed all statistical analysis using Prism (GraphPad Software). All error bars indicate standard errors of the mean (s.e.m). All *t* tests are two-tailed unpaired *t* tests. Time courses curves were analyzed by two-way ANOVA.

Supplementary Material

Refer to Web version on PubMed Central for supplementary material.

Acknowledgments

We thank N. Pace for advice on phylogenetic analysis, Y. Shi and members of the Xue laboratory for comments and discussions, L. Yang, H.W. Yang and C.L. Sun for technical support, and M. Driscoll (Rutgers University) for the *bzIs8* strain. This work was supported by NIH R01 grants (GM059083 and GM079097) and a Burroughs Welcome Fund Award to D.X. and a grant from MEXT of Japan to S.M. X.G. was supported by U. Colorado Matching Grant to the SCR Training Grant (T32 GM08759).

Abbreviations

AA	amino acid
GFP	green fluorescent protein
L1-L4	larval stages 1-4
N2	wild-type <i>C. elegans</i> strains-Bristol isolate
PCD	programmed cell death
RT-PCR	reverse transcriptase polymerase chain reaction
WT	wild type
CED	cell death abnormal
s.e.m	standard error of the mean

References

1. Gumienny TL, Lambie E, Hartwig E, Horvitz HR, Hengartner MO. Genetic control of programmed cell death in the *Caenorhabditis elegans* hermaphrodite germline. *Development*. 1999; 126:1011–1022. [PubMed: 9927601]
2. Gartner A, Boag PR, Blackwell TK. Germline survival and apoptosis. *WormBook*. 2008:1–20. [PubMed: 18781708]
3. Andux S, Ellis RE. Apoptosis maintains oocyte quality in aging *Caenorhabditis elegans* females. *PLoS Genet*. 2008; 4:e1000295. [PubMed: 19057674]
4. Gartner A, Milstein S, Ahmed S, Hodgkin J, Hengartner MO. A conserved checkpoint pathway mediates DNA damage--induced apoptosis and cell cycle arrest in *C. elegans*. *Mol Cell*. 2000; 5:435–443. [PubMed: 10882129]
5. Shi Y. Mechanisms of caspase activation and inhibition during apoptosis. *Mol Cell*. 2002; 9:459–470. [PubMed: 11931755]
6. Boatright KM, Salvesen GS. Mechanisms of caspase activation. *Curr Opin Cell Biol*. 2003; 15:725–731. [PubMed: 14644197]
7. Deveraux QL, Reed JC. IAP family proteins--suppressors of apoptosis. *Genes Dev*. 1999; 13:239–252. [PubMed: 9990849]
8. Deveraux QL, Takahashi R, Salvesen GS, Reed JC. X-linked IAP is a direct inhibitor of cell-death proteases. *Nature*. 1997; 388:300–304. [PubMed: 9230442]
9. Roy N, Deveraux QL, Takahashi R, Salvesen GS, Reed JC. The c-IAP-1 and c-IAP-2 proteins are direct inhibitors of specific caspases. *EMBO J*. 1997; 16:6914–6925. [PubMed: 9384571]
10. Deveraux QL, Roy N, Stennicke HR, Van Arsdale T, Zhou Q, Srinivasula SM, et al. IAPs block apoptotic events induced by caspase-8 and cytochrome c by direct inhibition of distinct caspases. *EMBO J*. 1998; 17:2215–2223. [PubMed: 9545235]
11. Meier P, Silke J, Leever SJ, Evan GI. The *Drosophila* caspase DRONC is regulated by DIAP1. *Embo J*. 2000; 19:598–611. [PubMed: 10675329]
12. Hawkins CJ, Wang SL, Hay BA. A cloning method to identify caspases and their regulators in yeast: identification of *Drosophila* IAP1 as an inhibitor of the *Drosophila* caspase DCP-1. *Proc Natl Acad Sci USA*. 1999; 96:2885–2890. [PubMed: 10077606]
13. Geng X, Shi Y, Nakagawa A, Yoshina S, Mitani S, Xue D. Inhibition of CED-3 zymogen activation and apoptosis in *Caenorhabditis elegans* by caspase homolog CSP-3. *Nat Struct Mol Biol*. 2008; 15:1094–1101. [PubMed: 18776901]
14. Shaham S. Identification of multiple *Caenorhabditis elegans* caspases and their potential roles in proteolytic cascades. *J Biol Chem*. 1998; 273:35109–35117. [PubMed: 9857046]
15. Cohen GM. Caspases: the executioners of apoptosis. *Biochem J*. 1997; 326:1–16. [PubMed: 9337844]
16. Blumenthal T. Trans-splicing and operons. *WormBook*. 2005:1–9. [PubMed: 18050426]
17. Ellis RE, Jacobson DM, Horvitz HR. Genes required for the engulfment of cell corpses during programmed cell death in *Caenorhabditis elegans*. *Genetics*. 1991; 129:79–94. [PubMed: 1936965]
18. Hengartner MO, Ellis RE, Horvitz HR. *Caenorhabditis elegans* gene ced-9 protects cells from programmed cell death. *Nature*. 1992; 356:494–499. [PubMed: 1560823]
19. Praitis V, Casey E, Collar D, Austin J. Creation of low-copy integrated transgenic lines in *Caenorhabditis elegans*. *Genetics*. 2001; 157:1217–1226. [PubMed: 11238406]
20. Tenenhaus C, Subramaniam K, Dunn MA, Seydoux G. PIE-1 is a bifunctional protein that regulates maternal and zygotic gene expression in the embryonic germ line of *Caenorhabditis elegans*. *Genes Dev*. 2001; 15:1031–1040. [PubMed: 11316796]
21. Xue D, Shaham S, Horvitz HR. The *Caenorhabditis elegans* cell-death protein CED-3 is a cysteine protease with substrate specificities similar to those of the human CPP32 protease. *Genes Dev*. 1996; 10:1073–1083. [PubMed: 8654923]

22. Rotonda J, Nicholson DW, Fazil KM, Gallant M, Gareau Y, Labelle M, et al. The three-dimensional structure of apopain/CPP32, a key mediator of apoptosis. *Nat Struct Biol.* 1996; 3:619–625. [PubMed: 8673606]
23. Sulston JE, Horvitz HR. Post-embryonic cell lineages of the nematode, *Caenorhabditis elegans*. *Dev Biol.* 1977; 56:110–56. [PubMed: 838129]
24. Brenner S. The genetics of *Caenorhabditis elegans*. *Genetics.* 1974; 77:71–94. [PubMed: 4366476]
25. Riddle, DL.; Blumenthal, T.; Meyer, BJ.; Preiss, JR. *C. elegans* II. Cold Spring Harbor Laboratory Press; Cold Spring Harbor, New York: 1997.
26. Harbinder S, Tavernarakis N, Herndon LA, Kinnell M, Xu SQ, Fire A, et al. Genetically targeted cell disruption in *Caenorhabditis elegans*. *Proc Natl Acad Sci USA.* 1997; 94:13128–13133. [PubMed: 9371811]
27. Gengyo-Ando K, Mitani S. Characterization of mutations induced by ethyl methanesulfonate, UV, and trimethylpsoralen in the nematode *Caenorhabditis elegans*. *Biochem Biophys Res Commun.* 2000; 269:64–69. [PubMed: 10694478]
28. Darland-Ransom M, Wang X, Sun CL, Mapes J, Gengyo-Ando K, Mitani S, et al. Role of *C. elegans* TAT-1 protein in maintaining plasma membrane phosphatidylserine asymmetry. *Science.* 2008; 320:528–531. [PubMed: 18436785]
29. Wang X, Wang J, Gengyo-Ando K, Gu L, Sun CL, Yang C, et al. *C. elegans* mitochondrial factor WAH-1 promotes phosphatidylserine externalization in apoptotic cells through phospholipid scramblase SCRM-1. *Nat Cell Biol.* 2007; 9:541–549. [PubMed: 17401362]
30. Yan N, Chai J, Lee ES, Gu L, Liu Q, He J, et al. Structure of the CED-4-CED-9 complex provides insights into programmed cell death in *Caenorhabditis elegans*. *Nature.* 2005; 437:831–837. [PubMed: 16208361]

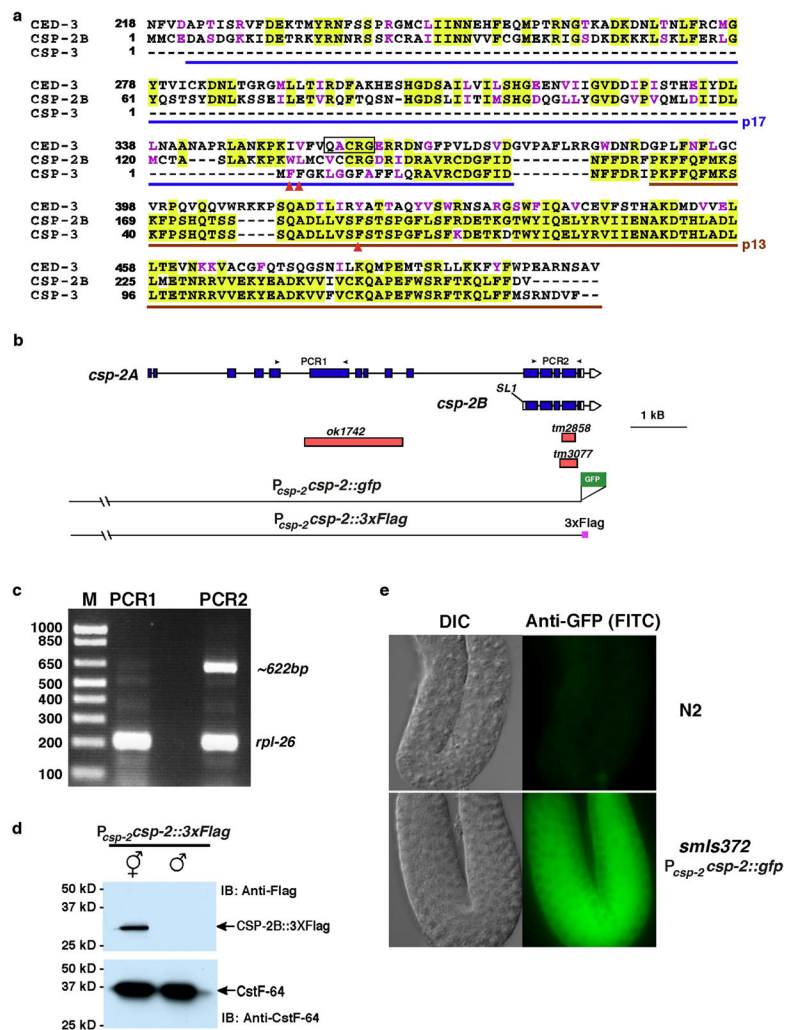


Figure 1. CSP-2, a CED-3 homologue, is expressed specifically in hermaphrodite germ cells. **(a)** Sequence alignment of CED-3, CSP-2B, and CSP-3. Residues that are identical are shaded in yellow and residues that are similar in pink. Trp131, Leu132, and Phe 186 of CSP-2B are indicated with red arrowheads. Underlines delineate the large and small subunits of CED-3, respectively. The box indicates the active-site pentapeptide of CED-3. **(b)** The *csp-2* gene structure and deletion mutations. Exons are depicted as boxes and introns as lines. The translated regions of *csp-2* are highlighted in blue. Three red boxes indicate the regions of *csp-2* removed by the three *csp-2* deletions, respectively. SL1 stands for SL1 trans-spliced leader sequence. **(c)** RT-PCR analysis of the relative abundance of CSP-2A and CSP-2B transcripts. Reverse transcription was performed on poly(A)_n mRNA isolated from mix-stage wild-type animals, followed by PCR amplification with primers specific to the CSP-2A coding region (PCR1 in **b**), or primers in the CSP-2A/2B coding region (PCR2 in **b**), or primers specific for a control gene *rpl-26* (encoding a large ribosomal subunit L26 protein). In the PCR1 lane, the predicted 706-bp CSP-2A-specific RT-PCR product was not seen. In the PCR2 lane, amplification of the 622-bp product corresponding to the

CSP-2A/2B transcript was detected. **(d)** Western blot analysis of $P_{csp-2csp-2::3xFlag}$ transgenic animals. 25 $P_{csp-2csp-2::3xFlag}$ transgenic hermaphrodites or males were solubilized in SDS sampling buffer and resolved on 15% SDS polyarylamide gel. The CstF-64 protein was used as a loading control. **(e)** *csp-2* is specifically expressed in *C. elegans* germ cells. Differential interference contrast (DIC) and anti-GFP immuno-staining images of exposed gonads of wild type (N2) and *smIs372* ($P_{csp-2csp-2::gfp}$) hermaphrodite animals are shown.

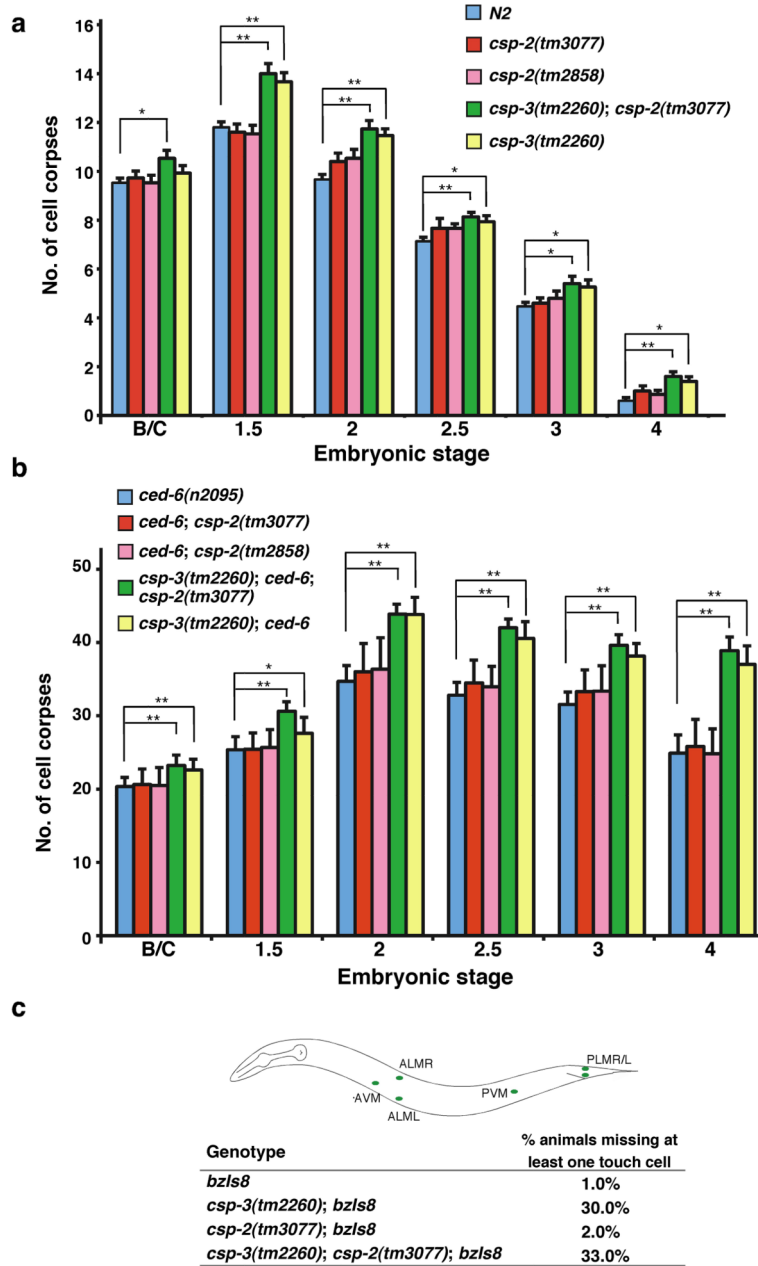


Figure 2.

Inactivation of *csp-2* does not affect apoptosis in somatic cells. (**a**, **b**) Embryonic cell corpse assays. Cell corpses were scored in the indicated strains. The *ced-6(n2095)* allele was used in **b**. Bean (B/C), 1.5-fold (1.5), 2-fold (2), 2.5-fold (2.5), 3-fold (3) and 4-fold (4) stage embryos were scored. The y axis represents the average number of cell corpses scored. Error bars are standard errors of mean (s.e.m.) At least 15 embryos were scored for each stage. The significance of differences between different genetic backgrounds was determined by unpaired *t* tests. *, $P < 0.05$; **, $P < 0.0001$. (**c**) Inactivation of *csp-2* does not cause ectopic death of touch receptor neurons. An integrated transgene (*bzIs8*) was used to monitor the survival of six touch receptor neurons (green circles) as described in Materials and Methods.

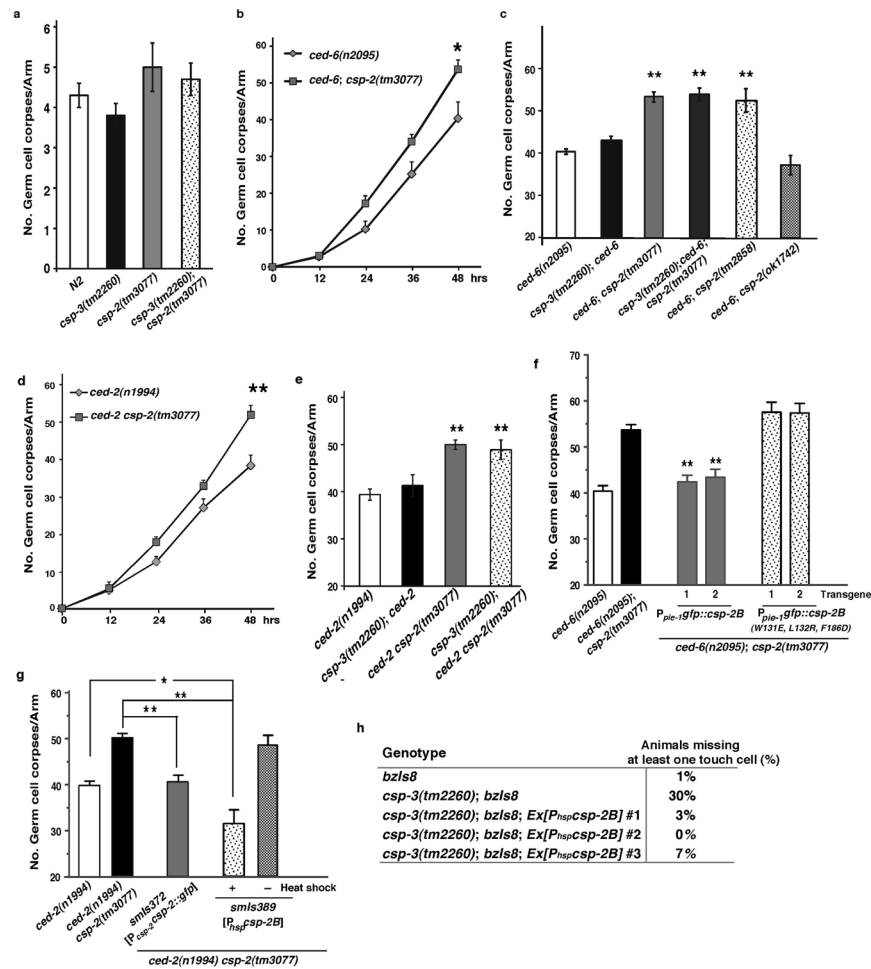
The percentages of animals missing one or more touch cells are shown. At least 100 animals were scored for each strain.

Author Manuscript

Author Manuscript

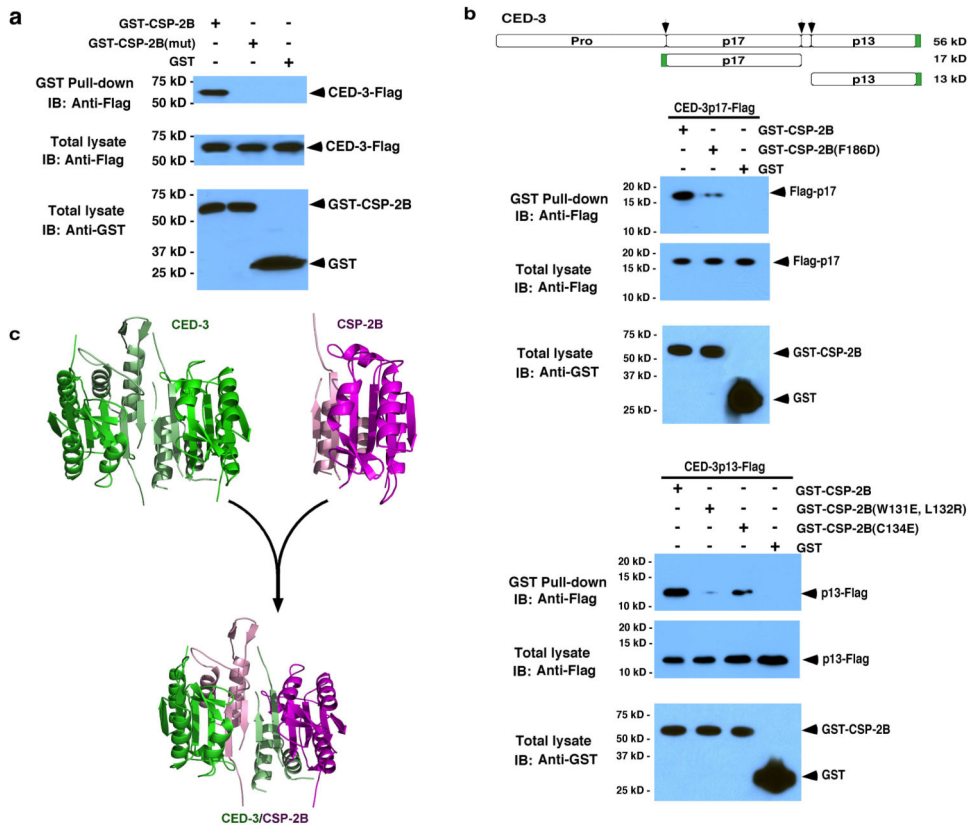
Author Manuscript

Author Manuscript

**Figure 3.**

Loss of *csp-2* causes increased apoptosis in germ cells. Germ cell corpses were scored in the indicated strains from one gonad arm 48 hours post L4 to adult molt (**a**, **c**, **e**, **f** and **g**) or every 12 hours post L4 to adult molt (**b** and **d**). Average numbers of germ cell corpses are shown. Error bars represent the standard errors of mean (s.e.m). At least 15 animals were scored in each strain or time point. In **b**, the significance of difference between *ced-6(n2095)* and *csp-2(tm3077); ced-6(n2095)* animals was determined by two-way analysis of variance (ANOVA). *, $P < 0.05$ for the whole time course. In **c**, the significance of differences between various *csp; ced-6(n2095)* strains and the *ced-6(n2095)* strain was determined by unpaired *t* tests. **, $P < 0.0001$. All other points had P values > 0.05 . In **d**, the significance of difference between *ced-2(n1994)* and *ced-2(n1994) csp-2(tm3077)* animals was determined by two-way ANOVA. **, $P < 0.0001$ for the whole time course. In **e**, the significance of differences between different *csp; ced-2(n1994)* strains and the *ced-2(n1994)* strain was determined by unpaired *t* tests. **, $P < 0.0001$. All other points had P values > 0.05 . (**f**, **g**) Rescue of the *csp-2* mutant by $P^{pie-1gfp::csp-2B}$, $P^{csp-2csp-2::gfp}$, or $P^{hsp::csp-2B}$ transgenes. The significance of differences between transgenic strains and the *ced-6(n2095); csp-2(tm3077)* strain (**f**), between transgenic strains and the *ced-2(n1994) csp-2(tm3077)* strain (**g**), or between the *smIs389*-containing strains and the *ced-2(n1994)* strain (**g**) was

determined by unpaired t tests. **, $P < 0.0001$. *, $P < 0.01$. All other points had P values > 0.05 . **(h)** The $P_{hsp}csp-2B$ transgenes rescue the missing cell defect of the $csp-3(tm2260)$ mutant. The presence of touch cells was scored as described in Figure 2c.

**Figure 4.**

CSP-2B associates with CED-3 *in vitro*. (a) CSP-2B binds to the CED-3 zymogen. GST-CSP-2B, GST-CSP-2B(mut), or GST was co-expressed in bacteria with the CED-3 zymogen tagged with a Flag epitope (CED-3-Flag). “mut” stands for W131E, L132R, and F186D substitutions. One portion of the soluble fraction was used in the western blot analysis to examine the expression levels of GST fusion proteins and CED-3-Flag using anti-GST and anti-Flag antibodies, respectively. The remaining portion of the soluble fraction was used in the GST fusion protein pull-down experiment and the amount of CED-3-Flag pulled down was analyzed by the western blot analysis using an anti-Flag antibody. (b) CSP-2B associates with both the large subunit and the small subunit of the CED-3 zymogen *in vitro*. The cartoon shows the domain structure of the CED-3 zymogen, with arrows indicating the three proteolytic cleavage sites that lead to the activation of the CED-3 zymogen. The large (p17) and the small (p13) subunits of CED-3 are shown below as boxes. The Flag epitope is labeled with green. GST-CSP-2B, GST-CSP-2B(F186D), GST-CSP-2B(W131E, L132R), GST-CSP-2B(C134E), or GST was co-expressed in bacteria with the CED-3 large subunit (Flag-p17) or the small subunit (p13-Flag), both of which are tagged with a Flag epitope. One portion of the soluble fraction was used in the western blot analysis to examine the expression levels of GST fusion proteins and CED-3 subunits using anti-GST and anti-Flag antibodies, respectively. The remaining portion of the soluble fraction was used in the GST fusion protein pull-down experiments and the amount of CED-3 subunits pulled down was analyzed by the western blot analysis using an anti-Flag antibody. (c) Structural model of the CED-3/CSP-2B complex. Because all caspases with known structures share a highly

conserved core structure, the structure of caspase-3 (PDB code 1pau) was used to represent the structures of CED-3 and CSP-2B. The large subunit of CED-3 is shown in green, the small subunit shown in lemon. The large subunit of CSP-2B is shown in magenta, the small subunit in light pink.

Author Manuscript

Author Manuscript

Author Manuscript

Author Manuscript

autoradiography. **(d)** A working model of how CSP-3 (left panel) and CSP-2B (right panel) inhibit CED-3 autoactivation and apoptosis in *C. elegans* somatic and germ cells, respectively.

Author Manuscript

Author Manuscript

Author Manuscript

Author Manuscript

Table 1The *csp-2* mutations cause reduced brood size

Genotype	Brood size ^a
<i>N2</i>	249 ± 28
<i>csp-2(tm3077)</i>	142 ± 31 ^b
<i>csp-2(tm2858)</i>	155 ± 19 ^b
<i>csp-2(ok1742)</i>	225 ± 27
<i>ced-9(n1653ts)</i>	22 ± 11
<i>ced-9(n1653ts); csp-2(tm3077)</i>	0.0 ± 0.4 ^c

^a All strains were maintained at 20°C, except that *ced-9(n1653ts)* and *ced-9(n1653ts); csp-2(tm3077)* strains were maintained at 25°C. Brood size was scored as the number of eggs laid by each hermaphrodite animal. Data shown are mean ± S.D. and are derived from three independent experiments. 20 animals were scored in each experiment.

^b Compared with *N2* animals, $P < 0.0001$ (two-tail student *t* test). Compared with *csp-2(ok1742)* animals, $P < 0.0001$ (two-tail student *t* test).

^c Compared with *ced-9(n1653ts)* animals, $P < 0.001$ (two-tail student *t* test).